Theoretical Study of Refrigerant Injection Technology Effect on Heat Pump Cycle Performance

Dr. Abdul Hadi N. Khalifa
Refrigeration and A/C Department, Middle Technical University/Baghdad
Email: ahaddi58@ya .com
Dr. Johain J. Faraj
Refrigeration and A/C Department, Middle Technical University/Baghdad
Hayder K. Hasan
Refrigeration and A/C Department, Middle Technical University/ Baghdad

Received on:16/6/2015 & Accepted on:29/9/2016

ABSTRACT

A 5 ton heat pump system with R22 was improved by Liquid Pressure Amplification (LPA) and refrigerant injection technologies. Three approaches for refrigerant injection were used. The first one was by mixture injection in suction line through accumulator; the second one was by liquid refrigerant injection through discharge line, while the third was a hybrid injection, in which vapour and liquid refrigerant were injected both simultaneously. For both approaches two and three LPA technique was used. The range of volume ratio of injected mixture and liquid was 1 to 7%, and 1 to 10% respectively, and in the hybrid injection, the volume ratio of injected mixture was 1 to 3% and for injected liquid was as mentioned above. The following improvement in cycle performance factors were achieved, for mixture injection 5.33%, for liquid injection 29.4%, and 33.45% for hybrid injection. The effect of condensing pressure on the cycle performance was studied also in this work.

Keyword: Refrigeration, Refrigerant injection, LPA technology, Heat pump

INTRODUCTION

For a number of years LPA technology is available in the market for Vapour Compression Refrigeration (VCR) systems with direct expansion evaporator, but has not as yet found wide-range applications [1]. LPA achieving energy efficiency in the VCR systems by reducing compressor discharge pressure, as well as, compression ratio [2]. In LPA systems, liquid refrigerant entering the liquid line is pressurized by centrifugal pump. The amount of pressurization is greater than the pressure drop through condenser. This permits the pressure of the condenser to be varied in line with variations of ambient temperature, leading to reduce the discharge pressures, during low ambient temperatures periods. Working at low condensing pressure reduces compressor power consumption and increases refrigeration capacity [1]. By increasing the pressure of liquid refrigerant, the associated saturation temperature is raised, while the actual temperature of the liquid constant. Therefore liquid becomes sub-cooled and will not flash if exposed to pressure drop in the liquid line.

De-superheating can be achieved by injection liquid refrigerant, from the same pump, into the discharge line; in such a way without affecting the refrigerant mass flow rate through the evaporation process. The injected liquid flashes into superheated vapour leading to reduce the discharge temperature closer to condensing temperature. As a result, less surface area in the condenser is required for de-superheating of vapour and more degree of sub-cooling. Fig. 1 shows LPA technology for VCR cycles [2]. Points (1-2-3-4) represent conventional VCR cycle and (a-b-c-d-e) represent VCR cycle with LPA technology.

https://doi.org/10.30684/etj.34.14A.16
2412-0758/University of Technology-Iraq, Baghdad, Iraq
This is an open access article under the CC BY 4.0 license http://creativecommons.org/licenses/by/4.0

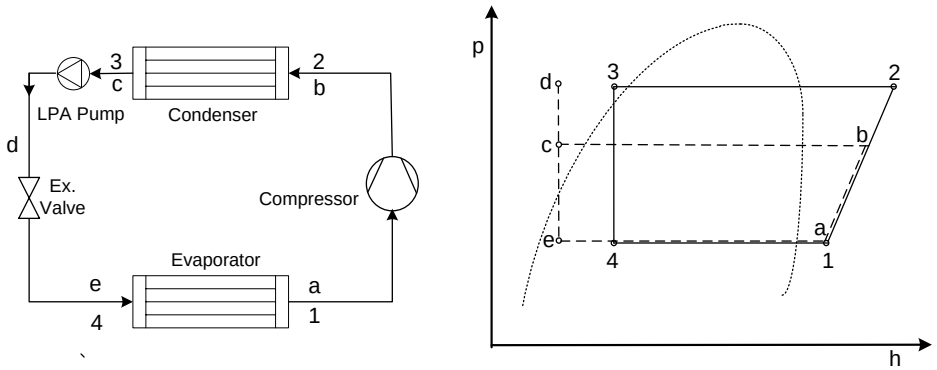

Figure (1) Schematic and p-h diagrams of the conventional VCR cycle With LPA technology [2]

A numerical study of scroll compressor to find exhaustive relationship between the performance of compressor and the injection parameters was done by Baolong et al. [3] [2007]. As a result, it was found that the injected scroll compressor gives the maximum indicated efficiency when the inner and outer compression ratio is right worth. Baolong Wang [4] [2010]: studied refrigerant injection technology for heat pump system with scroll compressor. One end of the injection circuit is located on two injection ports of the fixed scroll plate of the scroll compressor and the other connects with the outlet of the condenser. It was found that the refrigerant injection increases the heating / cooling capacity by 21.9% / 21.4% and enhances the heating COP / cooling EER (energy efficiency ratio) by 5.6% / 9.0%. The effect of compressor piston temperature on the cycle performance was studied by Sophie Colmek et al. [5] [2012]: the injection of vapour was realized on piston compressor. The compressor was enclosed in a room but not open to the ambient, so the compressor's temperature exceeded 130°C, which is limit temperature function of the compressor. A vapour injection was used with the help of capillary tube to reduce the temperature of the compressor on VCR. The quantity of vapour injection was sufficient to reduce the temperature, and not damage the system's capacity. The effect of internal leakage on the performance of variable speed scroll compressor was analysed by Cho et al [6] [2003]. It was found that the injection of refrigerant at the low operating frequency reduces the compressor performance due to the high leakage through the gap in the scroll wrap. The results showed that the capacities with the liquid injection decrease by 0.3~7.5% for the frequency of 45 Hz upon different injection ratios, but the capacity increases by 5.0~6.5% at the frequency of 105 Hz. Overall, the COP decreases by 9~19% at 45 Hz, and at 105 Hz; increases 5~9%, as compared to the non-injection case. The use of LPA in dairy plant was studied by A. Hadawey [1] [2008]. In which two LPA pumps were used with refrigerant R404A; the first one was installed after condenser for reducing condensing pressure, while the other one was used for liquid refrigerant injection. The discharge pressure dropped from 17 to 9.8 bar, compressor work was reduced by 26% and the refrigerating effect was increased by 35%. The discharge temperature was reduced by 31%. The effect of using LPA with a direct expansion R-22 package unit was studied by V. Vakiloroaya [2] [2014]: The results show that the average refrigerant discharge pressure drops from 17.5 to 11.7 bar after using an LPA pump whilst the refrigerant discharge temperature is reduced by 23.56 with electricity saving of around 25.3% on average. Khalifa, faraj and Adnan [7], investigated the effects of hybrid liquid and vapour refrigerant injections on a heat pump system using R407C refrigerant since it is more appropriate for Iraqi climate. It was found that the enhancement in performance factor varied from 35% at 14 °C to 28% at 8 °C.

System Simulation:

The main components of the suggested heat pump that is shown in Figure (2), were, a compressor, a condenser, an expansion device, an LPA Pump and an evaporator were modeled to simulate the overall cycle. The energy analysis is based on the first law of thermodynamic. The performance of a modified Heat Pump system was presented in terms of Performance Factor (PF), which defined as the ratio of heating capacity to the work done by the compressor. It is expressed as:

$$PF = \frac{Q_{cond.}}{W_{comp.}} \quad (1)$$

For a scroll type compressor, Klein and Reindl, (1997) [8], show that the thermal efficiency of the compressor is related to a pressure ratio and a temperature ratio by the following relationship;

$$\eta_{comp} = -60.25 - 3.814p_r - 0.0281{p_r}^2 + 111.3T_r - 50.31{T_r}^2 + 3.061p_rT_r \quad (2)$$

where:

$$p_r = \text{pressureratio} = \frac{P_{cond}}{P_{evap}} \quad (3)$$

$$T_r = \text{temperature ratio} = \frac{T_{sat.cond}}{T_{sat.evap}} \quad (4)$$

Mass flow rates associated with the processes of suction, discharge and flank leakage are estimated by Evandro and Deschamps [9].

$$\dot{m}_r = C_c A_i \sqrt{2p_{cond}\rho_2} \sqrt{\frac{\gamma}{\gamma-1}\left[\left(\frac{p_{evap}}{p_{cond}}\right)^{\frac{2}{\gamma}} - \left(\frac{p_{evap}}{p_{cond}}\right)^{\frac{\gamma+1}{\gamma}}\right]} \quad (5)$$

The overall heat exchanged between the first fluid (refrigerant) and the other fluid (Air) depends on the effectiveness of the heat exchanger (Condenser and Evaporator) and the heat capacity of the fluids [10]:

$$Q = \epsilon\, C_{min}(T_{h,i} - T_{c,i}) \quad (6)$$

Where:

ϵ = heat exchanger effectiveness which is defined as the ratio between the actual heat transfer to the maximum possible heat transfer:-

$$\epsilon = \frac{\dot{Q}}{\dot{Q}_{max}} \quad (7)$$

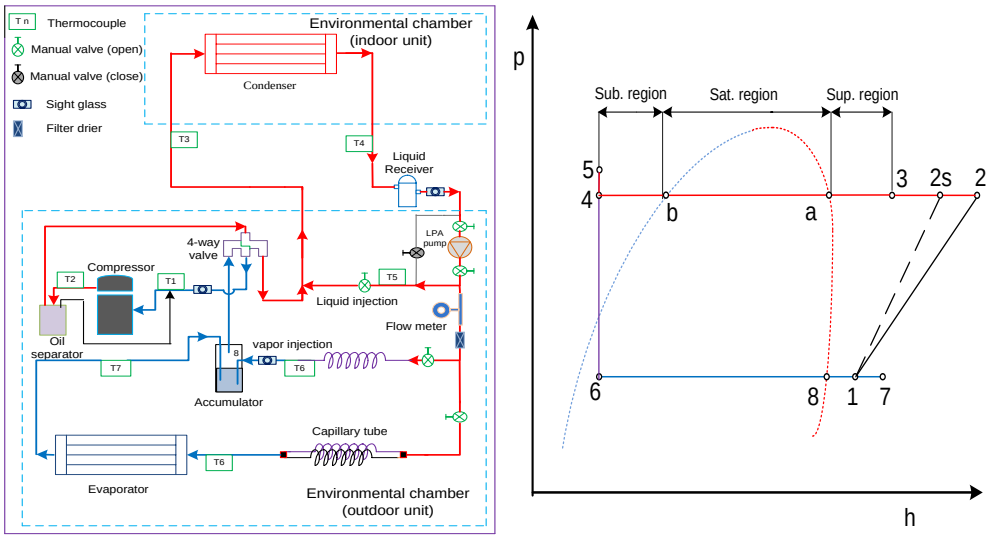

Figure (2) Schematic and P-h diagrams of heat pump system with LPA and hybrid injection technologies

Heat exchanger effectiveness depends on the temperature distribution of the fluids and paths of the fluids where the heat transfer takes place. The correlation of Kakac et al [10] is used to calculate the effectiveness of heat exchanger:

$$\epsilon = 1 - e^{\left\{\left(\frac{1}{C_r}\right)NTU^{0.22}\left[\exp\left(-C_r(NTU^{0.78})\right)-1\right]\right\}} \quad (8)$$

Where: C_r= heat capacity ratio $= \frac{C_{min}}{C_{max}}$ (9)

In the saturated region, the heat capacity on the refrigerant side approaches to infinity and C_r goes to zero. Thus; for this region the effectiveness is (Incropera and DeWitt) [11]:

$$\epsilon = 1 - e^{-NTU} \quad (10)$$

The NTU is the number of transfer units and it's given by:

$$NTU = \frac{UA}{C_{min}} \quad (11)$$

Where A is the heat transfer area at which U is based. The overall heat transfer coefficient between the refrigerant side (without fins), and finned air side is given as [10]:

$$UA = \left(\frac{1}{\eta_{s.a}\overline{h_a}A_a} + \frac{1}{\overline{h_r}A_r}\right)^{-1} \quad (12)$$

To determine the overall surface efficiency, it is required to determine the fins efficiency as if they existed alone. For staggered tubes, plate heat exchanger, the plates can be divided into hexagonal fins as shown in Figure (3). The hexagonal fin is analysed by Emma [12]; she treated the fins as circular fins, by determining an equivalent radius of hexagonal fin. This radius becomes equal to that of circular fin. The empirical relation for the equivalent radius is given by,

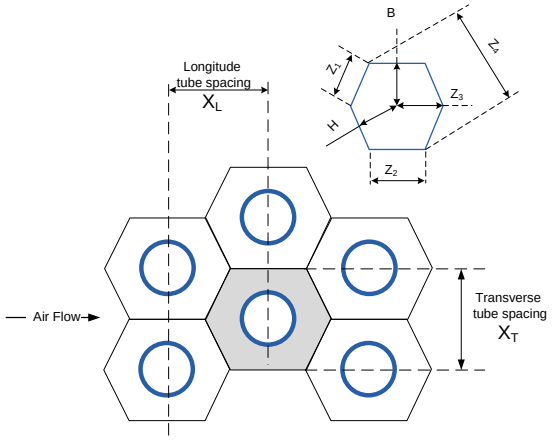

Figure (3) Hexagonal fin layout and tube array

$$\frac{R}{r_o} = 1.27\Psi(\beta - 0.3)^{1/2} \quad (13)$$

The coefficients Ψ and β are defined as:

$$\Psi = \frac{X_T}{D_o} \quad (14)$$

$$\beta = \frac{1}{X_T}\left(X_L^2 + \frac{X_T^2}{4}\right)^{1/2} \quad (15)$$

The equivalent radius of the circular fin R can be used to calculate the efficiency parameter of the fin by using the relationship of regular circular fin [11];

$$\phi = \left(\frac{R}{r_o} - 1\right)\left(1 + 0.35\ln\left(\frac{R}{r_o}\right)\right) \quad (16)$$

The air side surface efficiency is defined by Incropera and Dewitt [10] as follows:-

$$\eta_{s.a} = 1 - \frac{A_{fin}}{A_o}(1 - \eta_{fin}) \quad (17)$$

The circular fin efficiency η_{fin} is expressed as:

$$\eta_{fin} = \frac{\tanh(m_{es} R\phi)}{(m_{es} R\phi)} \quad (18)$$

The standard extended surface parameter (m_{es}) can be expressed as

$$m_{es} = \left(\frac{2\overline{h_a}}{k_f \delta_f}\right)^{1/2} \quad (19)$$

For this analysis,

$$B = X_L \text{ if } X_L < {}^{X_T}/_2 \text{ other wise } B = {}^{X_T}/_2 \quad (20)$$

$$H = \frac{1}{2}\sqrt{\left(\frac{X_T}{2}\right)^2 + {X_L}^2} \quad (21)$$

In Schmidt's study it is claimed that this approximation is valid for β >1. Zeller & Grewe (1994) [12] improved the equation of equivalent radius of circular fin by using relative perimeters of the hexagon and circle:

$$\frac{R}{r_o} = \frac{P_{hex}}{2\,\pi\, r_o} \quad (22)$$

Where: P_{hex} is the perimeter of the hexagonal fin

$$P_{hex} = 4z_1 + 2z_2 \quad (23)$$

The lengths z_1 and z_2, shown in Fig. 3, can be found by iterative solving of the following four equations:

$${z_2}^2 + (2B)^2 = {z_4}^2 \quad (24)$$

$$\left(\frac{z_1}{2}\right)^2 + H^2 = \left(\frac{z_4}{2}\right)^2 \quad (25)$$

$$H^2 + \left(\frac{z_1}{2}\right)^2 = \left(z_3 + {}^{z_2}/_2\right)^2 \quad (26)$$

$${z_1}^2 = {z_3}^2 + B^2 \quad (27)$$

Perrotin & Clodic (2003) [13], modified fin efficiency parameter φ with error not exceeding 2%, range of conditions $R/r_o \leq 6$ and $m_{es}(R\text{-}r_o) \leq 2.5$ for plain fins:

$$\varphi_m = \left(\frac{R}{r_o} - 1\right)\left[1 + \left(0.3 + \left(\frac{m_{es}(R-r_o)}{2.5}\right)^{1.5 - \frac{R}{12\,r_o}}\left(0.26\left[\frac{R}{r_o}\right]^{0.3} - 0.3\right)\right) ln\left(\frac{R}{r_o}\right)\right] \quad (28)$$

Hong & Webb (1996) [14] modified fin efficiency equation to obtain better accuracy. Therefore the equation becomes:

$$\eta_{fin} = \frac{\tanh(m_{es} R\varphi_m)}{(m_{es} R\varphi_m)} cos(0.1\, m_{es} R\varphi_m) \quad (29)$$

Heat Transfer Correlations:

The condenser is divided into three regions: the first is the superheat region, the second is the two-phase region, and the third is subcooled region which is the last portion of condenser. On the other hand, the evaporator is divided into the two phase and the superheat regions. The heat transfer coefficient can be determined according to each region as follows:

Single Phase Regions (Superheated/Subcooled):

The heat transfer coefficients in the single phase region (Liquid or Vapour) for this study are calculated by the correlation of Petukhov-Kirillov, [14] which predicts the result in the range $10^4 < Re_b < 5 * 10^6$, $0.5 < Pr_b < 200$ within 5 to 6 % error:

$$Nu_b = \frac{\left(\frac{f_b}{2}\right) Re_b Pr_b}{1.07 + 12.7\left(\frac{f_b}{2}\right)^{\frac{1}{2}}\left(Pr_b^{\frac{2}{3}} - 1\right)} \quad (30)$$

Where:

f_b: Filonenko's friction factor which is given by [15]:

$$f_b = [1.58\ln(Re_b) - 3.28]^{-2} \quad (31)$$

3-2 Two Phase Regions (Boiling/Condensation):

The two phase heat transfer coefficient is calculated by a modified Cavallini's equations (Kondou and Hrnjak 2012) [16]:

$$h_{TP} = \left[h_A \left(\frac{J_G{}^T}{J_G}\right)^{0.8} - h_{strat}\right]\left(\frac{J_G}{J_G{}^T}\right) + h_{strat} \quad (32)$$

Where:

J_G , $J_G{}^T$: Dimensionless vapour velocities are calculated by:

$$J_G = \frac{X_b G_r}{\sqrt{g d_i \rho_{Vsat}(\rho_{Lsat} - \rho_{Vsat})}} \quad (33)$$

$$J_G{}^T = \left[\left(\frac{7.5}{4.3X_{tt}{}^{1.111} + 1}\right)^{-3} + 2.6^{-3}\right]^{-\frac{1}{3}} \quad (34)$$

Pr_{L_f}= Prandtl Number of liquid at film temperature is given by:

$$Pr_{L\_f} = \frac{\overline{Cp_L}\,\mu_{L-f}}{k_{L-f}} \quad (35)$$

The average specific heat of liquid ($\overline{Cp_L}$) can be express as:

$$\overline{Cp_L} = \frac{h_{Lsat} - h_{L,wi}}{T_{sat} - T_{wi}} \quad (36)$$

h_{strat} = Fully-stratified heat transfer coefficient $\left(\frac{W}{m^2 k}\right)$ express as:

$$h_{strat} = 0.725\left[\frac{k_{Lf}{}^3 \rho_{Lf}(\rho_{Lf} - \rho_{V,sat}) g \Delta h_{LV}}{\mu_{Lf} d_i (T_{sat} - T_{wi})}\right]^{0.25}\left[1 + 0.741\left(\frac{1-X_b}{X_b}\right)^{0.3321}\right]^{-1} + \left[(1 - X_b{}^{0.087})h_{LO\_f}\right] \quad (37)$$

h_{LO_f} = liquid only heat transfer coefficient at film temperature, is calculate by using Dittus-Boelter equation [17]:

$$h_{LO\_f} = 0.023(Re_{L\_f})^{0.8} Pr_{L\_f}{}^{0.4}\left(\frac{k_{Lsat}}{d_i}\right) \quad (38)$$

$$h_A = h_{Lf}\left[1 + 1.128X_b{}^{0.8170}\left(\frac{\rho_{Lsat}}{\rho_{Vsat}}\right)^{0.3685}\left(\frac{\mu_{Lsat}}{\mu_{Vsat}}\right)^{0.2363}\left(1 - \frac{\mu_{Vsat}}{\mu_{Lsat}}\right)^{2.144} Pr_{L\_f}{}^{-0.1}\right] \quad (39)$$

The Martinelli parameter (X_{tt}) can express as [18]:

$$X_{tt} = \left(\frac{1}{X_b} - 1\right)^{0.9}\left(\frac{\rho_{Vsat}}{\rho_{Lsat}}\right)^{0.5}\left(\frac{\mu_{Lsat}}{\mu_{Vsat}}\right)^{0.1} \quad (40)$$

All the above mentioned relations constitute a complete set of nonlinear algebraic equations that should be solved simultaneously in order to predict system performance under different operating conditions. These equations relay extensively on air and refrigerant thermal and thermo-physical properties. The most efficient software to handle this problem is the Engineering Equation Solver (EES for short) program since it has built in capabilities of calculating fluid properties easily. Thus the EES was adopted to solve this system of equations according to the flow chart shown in figure (4).

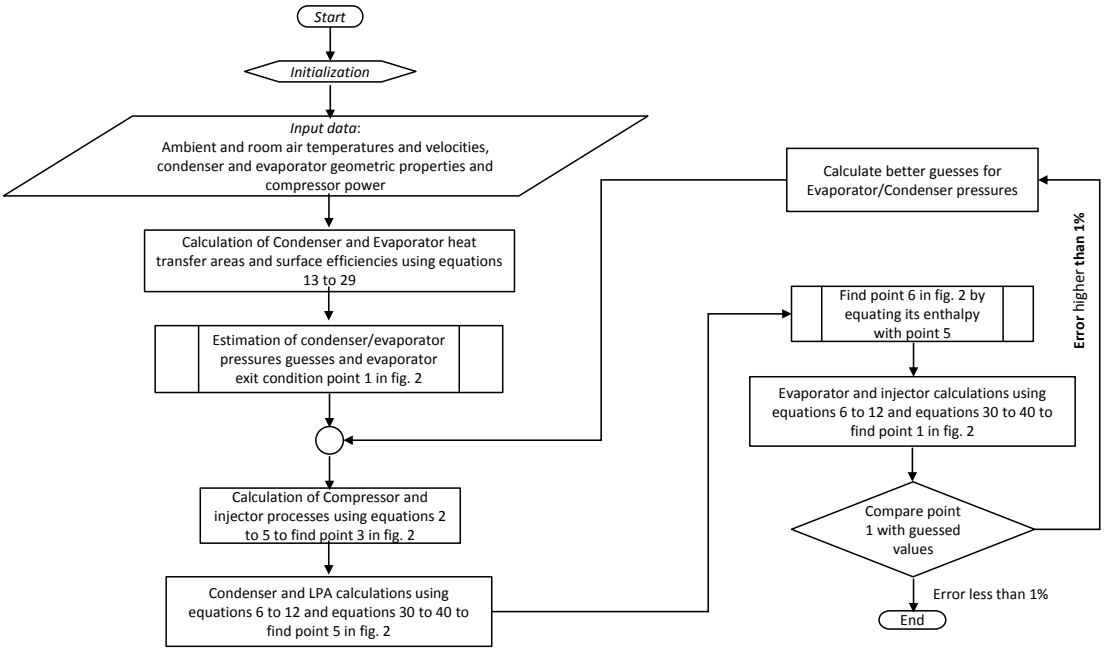

Figure (4) Flow chart of problem

Results and Discussions:

The heat transfer coefficients in condenser regions versus condensing pressure are shown in Figures (5) and (6). It can be seen from the figures that the heat transfer coefficients for single phases increase with the increasing of condensing pressure, as a result of increase in the density of refrigerant. While heat transfer coefficient for two phase region shows contrary trends, since one of the main parameters in calculation of heat transfer coefficient for two phase region is the latent heat of condensation, which decreases with increasing condensing pressure. Figure (7) shows the variation of condenser effectiveness with condensing pressure in three regions mentioned above. The figure shows that the effectiveness in these regions is varied inversely with condensing pressure, owing to increase in the temperature difference between the refrigerant side and air side; and a limited available area of condenser for heat transfer. Figure (8) shows the PF versus condensing pressure. Since as the pressure ratio decreases, the power consumed by compressor reduces also, therefore it can be seen from the figure that the PF decreases with increase in the condensing pressure. Accordingly the PF increases with the decrease in pressure ratio; the refrigerant-side pressure drop is effect proportional to the compressor power.

The pressure drop in the condenser occurs in the three regions of the condenser but the largest values in the two-phase region, as shown in Figure (9). Figure (10) shows the air side heat transfer coefficients versus the average air side temperature.

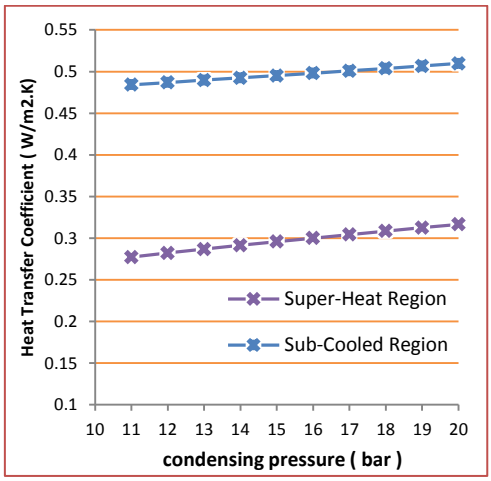

Figure (5) Variation of heat transfer coefficient in super-heat and sub-cooled regions vs condensing pressure

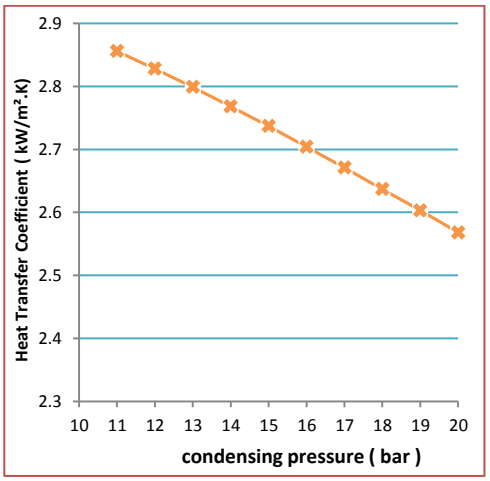

Figure (6) Variation of heat transfer coefficient in two-phase region vs condensing pressure

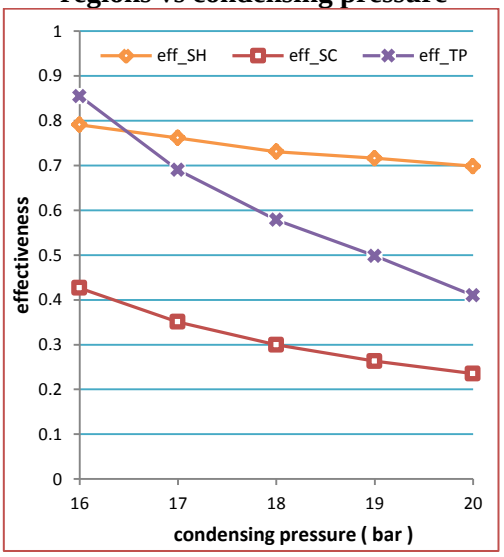

Figure (7) variation of condenser effectiveness vs condensing pressure

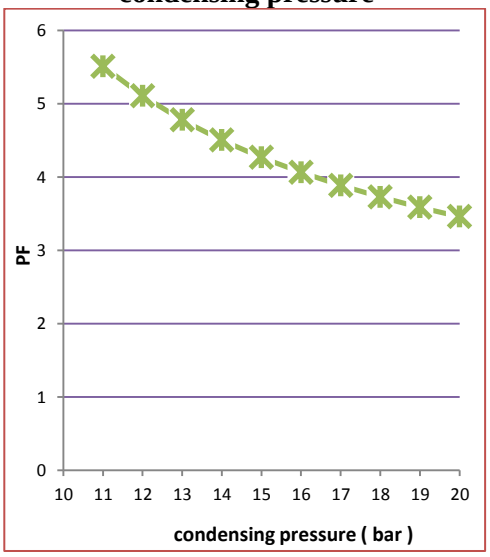

Figure (8) The variation of PF vs condensing pressure

It is observed from the figure; the air-side heat transfer coefficients have insignificant change with temperature changes, due to small change in the properties of air. The maximum difference between air side heat transfer coefficients (2.8%) when the air temperature changed from 20℃ to 65℃. Figure (11) shows the effect of air side temperature on the fin efficiency. The efficiency decreases when the air side temperature is increased. As the air-side temperature elevated the convective heat transfer coefficient increases as a consequence resulting in fin efficiency reduction. Figure (12) shows the effect of volume ratio of injected mixture (volume flow rate ratio of the injection to the main) on the heat pump PF. The figure shows that the PF increases by about 5.32% when the volume ratio of injected mixture is 5%. The PF tends to reduce as the ratio increases more than 5% due to decrease in the mass flow rate available for load in the evaporator.

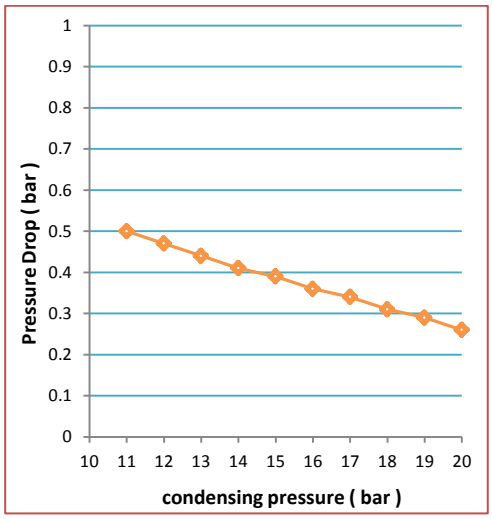

Figure (9) Refrigerant-side pressure drop vs condensing pressure

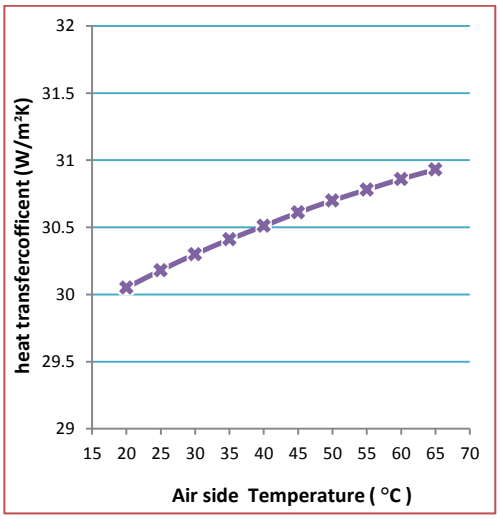

Figure (10) Air-side heat transfer coefficient vs ambient temperature

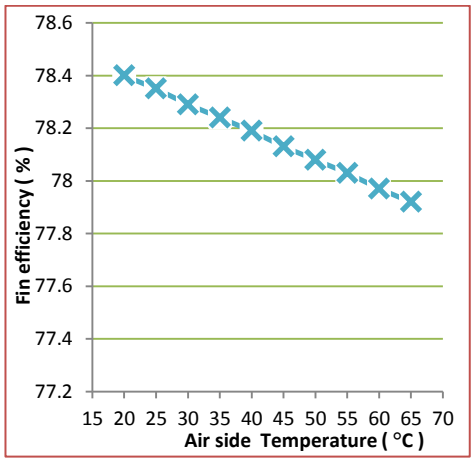

Figure (11) variation of fin efficiency vs average air-side temperature

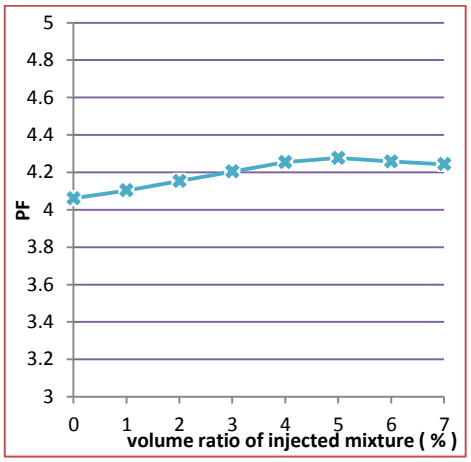

Figure (12) The variation of PF vs volume ratio of injected mixture

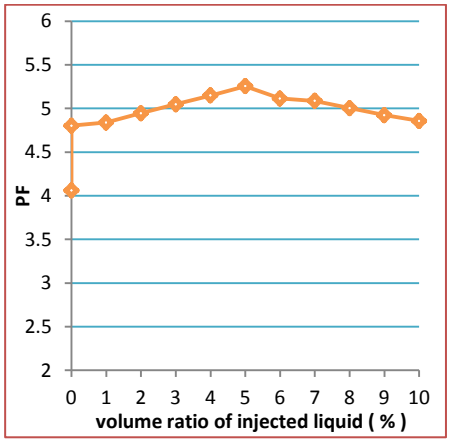

Figure (13) The variation of PF vs volume ratio of injected liquid

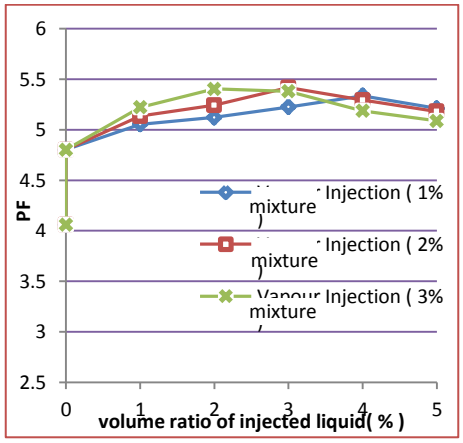

Figure (14) The variation of PF vs volume ratio of hybrid injection

Figure (13) shows the effect of LPA pump and volume ratio of injected liquid on the PF. It is observed from the figure the PF increases by about 18.27% by operating LPA pump in the cycle, without injected any refrigerant, and by about 29.4% as liquid is injected in the ratio of 5%, behind this ratio the heat pump PF reduces due to reduction in refrigerant mass flow rate through evaporator. Figure (14) shows the effect of hybrid injection on cycle PF versus volume ratio of injected liquid for different volume ratios of injected mixture, namely 1, 2 and 3%. It can be seen from the figure that, the PF for traditional Heat pump is about 4, as the LPA operate in the cycle, Pf increases to about 4.8. Also the figures show that the maximum PF is for injected liquid in the ratio of 3% with conjunct of 2% volume ratio of injected mixture.

CONCLUSIONS:

From the theoretical results it can be concluded that:

1- Increasing condensing pressure to 20 bar shows the following effects:

a- Increasing both heat transfer coefficients for superheated region and sub-cooled regions by about 14.2% and 5.3% respectively, while the heat transfer coefficient of two phase region is reduced by 10.1%.

b- Reducing cycle PF by 37.23%

c- The condensing pressure in Iraq should be in the range of 14 to 15 bar, this range gives maximum PF the cycle.

2- The best volume ratios of injected refrigerant are as follows:

a- 5% of injected mixture that gives cycle PF of 4.3.

b- 5% of injected liquid, in which the cycle PF equals 5.24.

c- 2% mixture and 3% liquid for hybrid injection, at these ratios the cycle PF equals 5.42.

REFERENCES:

[1] Hadawey, A., Y. T. Ge, and S. A. Tassou. "Energy Saving Through Liquid Pressure Amplification in a Dairy Plant Refrigeration System." CEBER Brunel University Uxbridge Middlesex, UB8 3PH, UK. (2008).

[2] Vakiloroaya, V., and Q. P. Ha. "Energy-Efficient Air-Cooled DX Air-Conditioning Systems with Liquid Pressure Amplification." University of Technology, Sydney, Australia, (2014).

[3] Wang, Baolong, Wenxing Shi, and Xianting Li. "Numerical analysis on the effects of refrigerant injection on the scroll compressor." *Applied Thermal Engineering* 29, no. 1 (2009): 37-46.

[4] Wang, B., Han, L., Shi, W., & Li, X. "A Novel Capacity Modulation Technology for Heat Pump System with Scroll Compressor." International Refrigeration and Air Conditioning Conference, Paper 1074. (2010).

[5] Colmek, Sophie, and Laurent Goderneaux. "Gas Vapor Injection on Refrigerant Cycle Using Piston Technology." International Refrigeration and Air Conditioning Conference. Paper 1220. (2012).

[6] Cho, H. H., and Y. Kim. "Experimental Study on an Inverter-Driven Scroll Compressor with an Injection System." International Compressor Engineering Conference at Purdue University, (2000):785-790.

[7] Abdual Hadi N. Khalifa, Johain j. faraj and Anmar Adnan, "Effect of Different Refrigerant Injection Techniques on Heat Pump cycle Performance", Eng. & Tech. Journal ,Vol.32, Part (A), No.10, 2014

[8] Klein, S. A. and Reindl, D. T, 1997. "The Relationship of Optimum Heat Exchanger Allocation and Minimum Entropy Generation for Refrigeration Cycles," Proceedings of the ASME Advanced Energy Systems Division(1997), vol. 37, pp. 87-94.

[9] Pereira, Evandro LL, and Cesar J. Deschamps. "A Lumped Thermodynamic Model for Scroll Compressors with Special Attention to the Geometric Characterization during the Discharge Process." International Compressor Engineering Conference. (2010).
[10] Kakac, Sadik, Hongtan Liu, and Anchasa Pramuan jaroenkij. "Heat Exchangers: Selection, Rating, and Thermal Design." CRC press, (2012).
[11] Frank P. Incropera , David P. DeWitt and Theodore L. Bergman," Introduction to heat transfer" 5th edition, Johan Willey and Sons, (2007)
[12] Sadler, Emma May. "Design Analysis of a Finned-Tube Condenser for a Residential Air-Conditioner using R-22." PhD Thesis, Georgia Institute of Technology, (2000).
[13] Perrotin, T., Clodic, D., 2003, Fin Efficiency Calculation in Enhanced Fin-and-Tube Heat Exchangers in Dry Conditions, 20th *International Congress of Refrigeration*, Washington-DC, USA . (2003).
[14] Petukhov, B. J. ; Kirillov, V. V. ; and Maidenik, V. N. : Heat Transfer Experimental Research for Turbulent Gas Flow in Pipes at High Temperature Difference Between Wall and Bulk Fluid Temperature. Proceedings of the Third International Heat Transfer Conference, Chicago, Aug. 7-12, 1966.
[15] Fang, Xiande, Yu Xu, and Zhanru Zhou. "New correlations of single-phase friction factor for turbulent pipe flow and evaluation of existing single-phase friction factor correlations." Nuclear Engineering and Design 241.3 (2011): 897-902.
[16] Kondou, C., Hrnjak, P.S. Condensation from Superheated Vapor Flow of R744 and R410A at Subcritical Pressures in a Horizontal Smooth Tube", Int. J. Heat Mass Transfer, (2012) , vol. 55: p. 2779–2791
[17] Kondou, Chieko, and Predrag S. Hrnjak. "Heat Rejection in Condensers: De-superheating, Condensation in Superheated Region and Two Phase Zone." University of Illinois, Department of Mechanical Science and Engineering ACRC, Urbana, IL, USA. (2012).
[18] Souza, A. L., et al. Pressure drop during two-phase flow of refrigerants in horizontal smooth tubes. Air Conditioning and Refrigeration Center. College of Engineering. University of Illinois at Urbana-Champaign., 1992.

Nomenclature

Latin Symbols:

Symbols	**Meaning**	**Units**
A_a	Air side heat transfer area	m^2
C	Heat capacity	kW
C_C	Contraction flow coefficient	---
c_p	Specific heat at constant pressure	kJ/kg.K
G	Mass velocity defined by ($\dot{m}/Area$)	kg/m^2 Sec
G	Acceleration due to Gravity	m/s^2
H	Specific enthalpy/ heat transfer coefficient	kJ/kg W/m^2.K
$\bar{h}$	Area average heat transfer coefficient	W/m^2 K
JG	Vapour mass velocity factor	---
Kf	Thermal conductivity of fin	W/m K
m_{es}	Fin standard extended surface parameter	---
$\dot{m}_r$	Refrigerant mass flow rate	kg/s
NTU	Number of transfer units	---
Nu	Nusselt number (h*D / k)	---
P_{hex}	Perimeter of the hexagonal fin	m
Pr	Prandtle number (Cp*μ/k)	---
Q	Total heat transfer rate	kW
R	Equivalent radius of fins	m
Re	Reynolds number (ρ*v*L/μ)	---

U	Overall heat transfer coefficient	$W/m^2.K$
X	Thermodynamic vapour quality	---
XL	Longitudinal tube spacing	m
XT	Transverse tube spacing	m
Xtt	Martinelli parameter	---

Greek Symbols:

Symbols	Meaning	Units
$_f\delta$	Fin thickness	m
γ	Modify angle	Rad
ϵ	Heat exchanger effectiveness	---
η_{comp}	Compressor thermal efficiency	%
$\eta_{s.a}$	Surface efficiency for air side	%
ρ	Fluid density	kg/m^3
μ	Viscosity	kg/m.sec
ϕ, φ_m	Fin efficiency parameters original and modified	---

Subscripts:

Symbols	Meaning
A	Air side
B	Properties at bulk temperature
c,i	Inlet cold fluid
comp.	Compressor
cond.	Condenser
F	Properties at film temperature
h,i	Inlet hot fluid
I	Inside
L	Liquid
LV	Difference between liquid and vapour properties
max	Maximum
min	Minimum
O	Out side
R	Refrigerant side
sat	Saturation condition
SC	Subcooled
SH	Superheated
V	Vapour
TP	Two phase
W	Properties at wall temperature